Polymer Chemistry

PAPER

Electronic Supplementary Information

Thermoresponsive Polymers as Macromolecular Coordination Ligands: Complexation-Dependence of Thermally Induced Aggregation in Aqueous Solution

Maximilian Felix Toni Meier[a], Franck Thetiot[b], Narsimhulu Pittala[b], Ingo Lieberwirth[c], Cleiton Kunzler[a], Smail Triki[b], and Ulrich Jonas*[a]

We have designed novel macromolecular coordination ligands (MCLs) by conjugation of thermoresponsive polymers based on poly(*N*-isopropylacrylamide) ($\bar{M}_n$ around 3 to 25 kg·mol^{-1}) with 1,2,4-triazole coordination sites. These triazole units were integrated into two fundamentally different MCL architectures *via* reversible addition-fragmentation chain transfer polymerization following two synthetic strategies:
(I) The customized chain transfer agent 1-{[3-(4*H*-1,2,4-triazol-4-yl)propyl]amino}-2-methyl-1-oxopropan-2-yl dodecyl carbonotrithioate (DMP-APTRZ) was employed for hemi-telechelic MCLs with a single triazole end group.
(II) A tailored comonomer *N*-[3-(4*H*-1,2,4-triazol-4-yl)propyl]methacrylamide (APTRZMAAm) provides access to multidentate MCLs with a controllable number of triazole side groups along the polymer backbone.
The thermally controlled variation of the MCL volume demand in aqueous solution was exploited for reversible aggregate formation upon Fe^{2+} complexation. Thermal response was studied *via* UV/Vis turbidity measurments, aggregate dimensions were determined *via* DLS, while the aggregate morphology was analyzed *via* customized TEM.

Keywords: Poly(*N*-Isopropylacrylamide) (PNIPAAm), 1,2,4-triazole-Fe^{2+} complex, RAFT polymerization, coordination monomer, thermoresponsive aggregation, macromolecular coordination ligand, self-assembly

CONTENT

1. Synthesis

1.1.Coordinating motive APTRZ

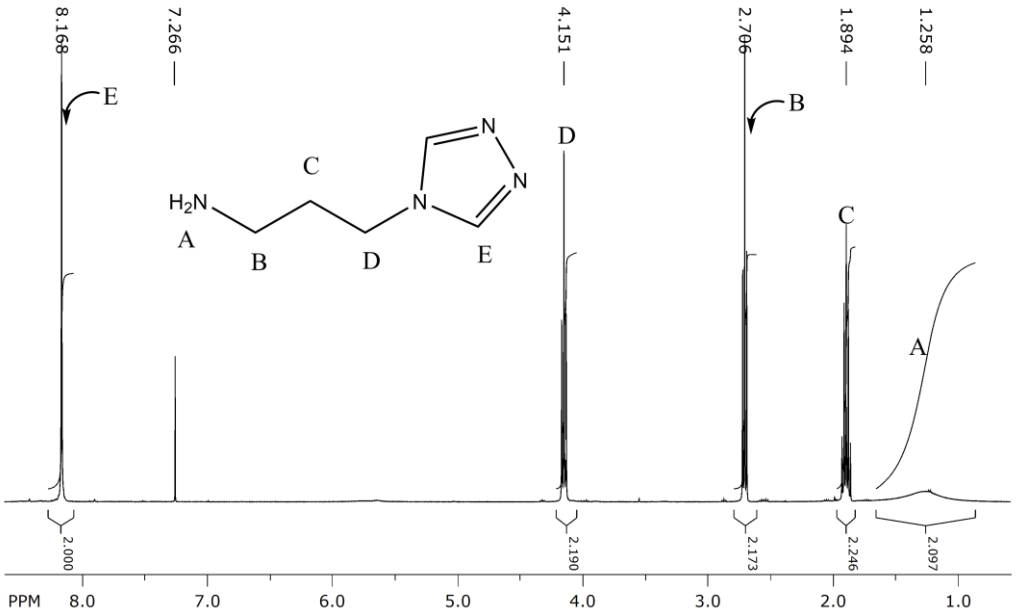

Figure S1: ^{1}H-NMR spectrum (500 MHz) of APTRZ, recorded in $CDCl_3$.

1.2.Chain Transfer Agent DMP

2-{[(Dodecylthio)carbothioyl]thio}-2-methylpropanoic acid (DMP) was synthesized according to a modified procedure of Postma et al.[41] 1-Dodecanethiol (3.83 g, 18.9 mmol, 4.5 mL) was dissolved in chloroform (50 mL) until TEA (2.85 g, 28.2 mmol, 3.9 mL) was added. The mixture was stirred for 20 minutes, before CS_2 (3.40 g, 37.6 mmol, 2.7 mL) was added through a septum forming a yellowish reaction mixture. After another 3 hours reaction time, α-bromoisobutyric acid (3.15 g, 18.9 mmol) was given to the reaction mixture. The product was obtained after 24 hours reaction time and threefold extraction with 1M HCl (100 mL) and water (100 mL). The product was dried over anhydrous sodium sulfate and concentrated to dryness. The product was recrystallized twice in cold hexane. The reaction status was monitored using the TLC (silica gel, EtOAc:Hex=1:2, R_f(DMP)=0.40, iodine indicator and $CHCl_3$:MeOH:NH_3=13:6:1, R_f(DMP)=0.28, iodine indicator).

Yield: 3.35 mg (50%)

^{1}H NMR (400 MHz, $CDCl_3$, shown in appendix Figure S2A), δ ppm: 0.89 (t, 3H, J=7.0 Hz, –CH_2-CH_3), 1.26 - 1.39 (m, 18H, -(CH_2)$_9$-CH_3), 1.68 (p, 2H, J=7.3 Hz, -CH_2-CH_2-(CH_2)$_9$-), 1.73 (s, 6H, -C-(CH_3)$_2$) and 3.29 (t, 2H, J=7.3 Hz, -CS_3-CH_2-).

^{13}C NMR (101 MHz, $CDCl_3$, shown in appendix Figure S2B), δ ppm: 14.1 (-CH_2-CH_3), 22.7 (-CH_2-CH_3), 25.2 (-C-(CH_3)$_2$), 27.8 (-(CH_2)$_8$-), 29.0 (-(CH_2)$_8$-), 29.1 (-(CH_2)$_8$-), 29.4 (-(CH_2)$_8$-), 29.5 (-(CH_2)$_8$-), 29.6 (-(CH_2)$_8$-), 29.6 (-(CH_2)$_8$-), 31.9 (-CH_2-CH_2-CH_3), 37.2 (-CS_3-CH_2-), 55.5 (-CS_3-C-(CH_3)$_2$-COOH), 178.9 (-COOH) and 220.8 (-CS_3-).

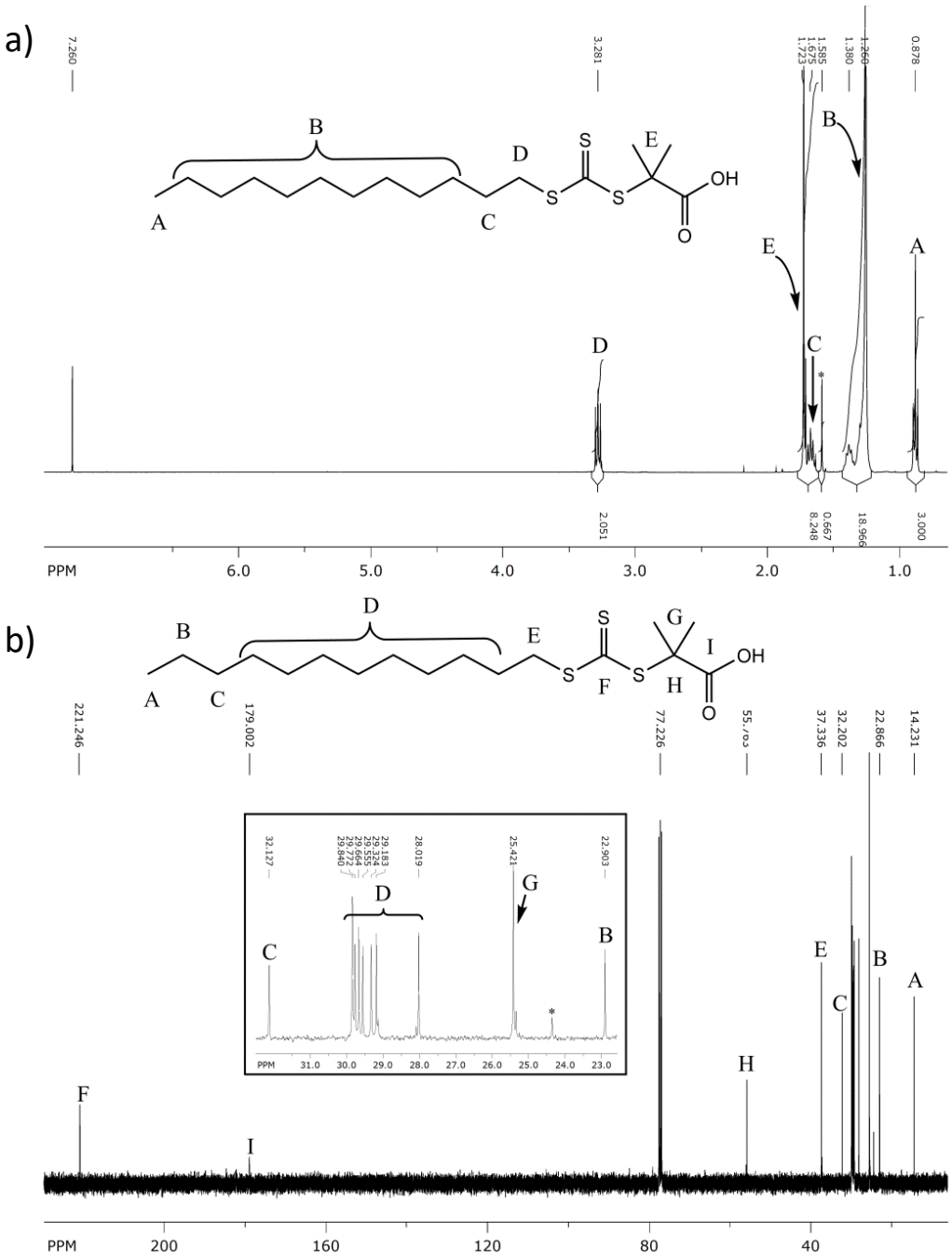

Figure S2: a) ^{1}H- (400 MHz) and b) ^{13}C-NMR (100 MHz) spectra of the synthesized, unmodified chain transfer agent DMP, recorded in $CDCl_3$. Asterisks mark solvent residues (H_2O).

1.3. Activation of Chain Transfer Agent DMP-NHS

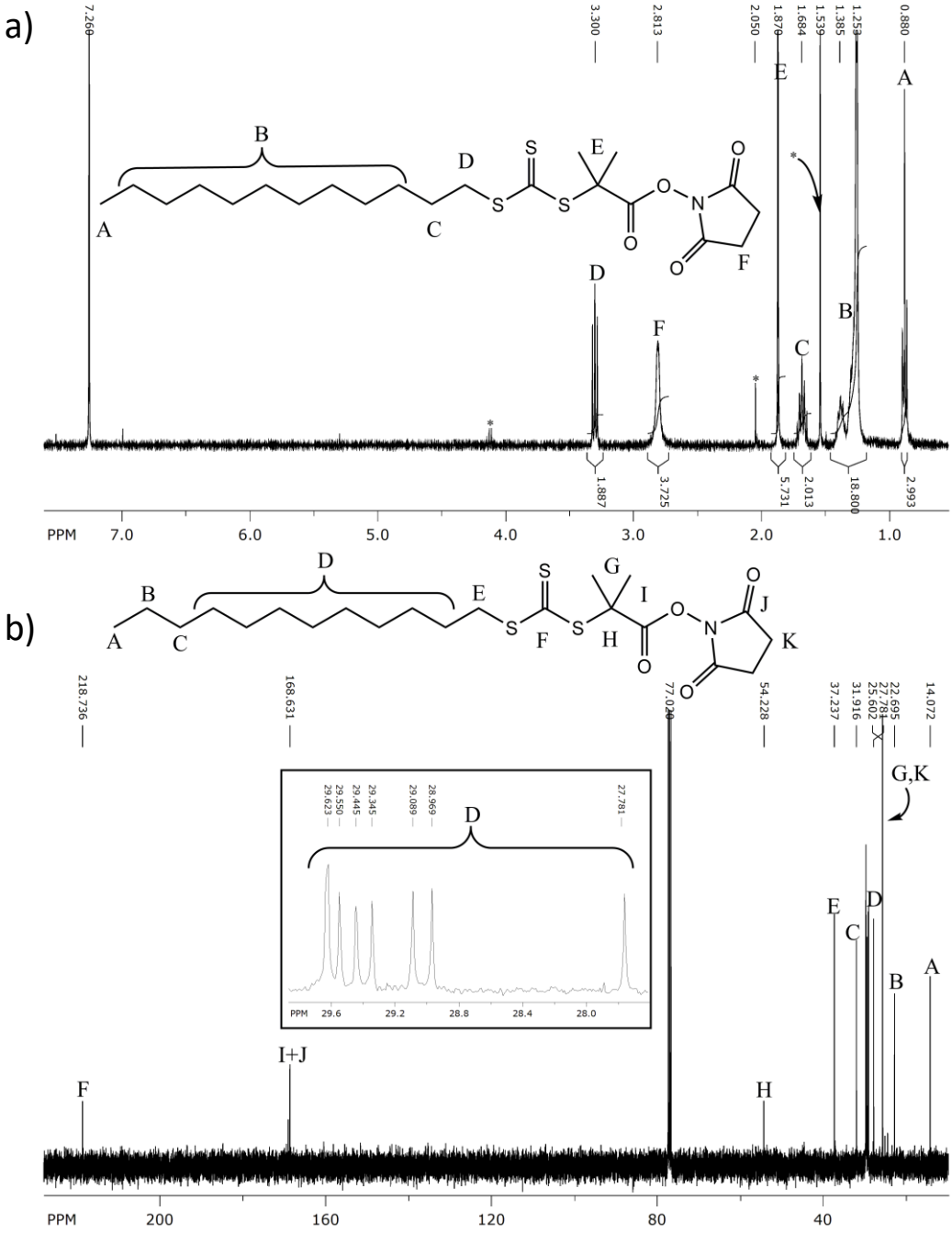

Figure S3: a) ^{1}H- (400 MHz) and b) ^{13}C-NMR (100 MHz) spectra of the activated chain transfer agent DMP-NHS, recorded in $CDCl_3$. Asterisks mark solvent residues (H_2O).

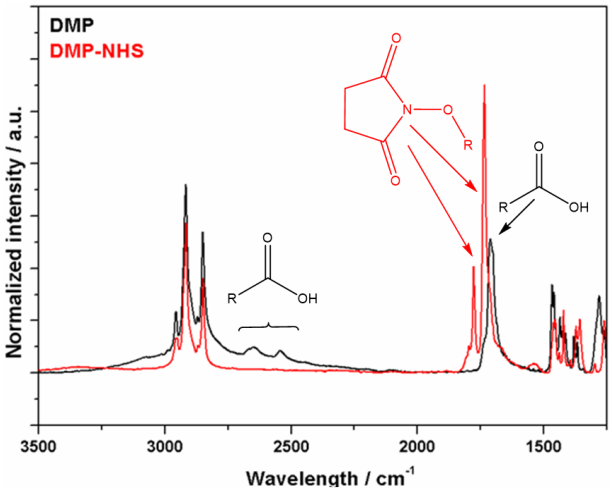

Figure S4: ATR-IR spectra of the unmodified educt DMP (black) and activated chain transfer agent DMP-NHS (red).

1.4.Triazole Chain Transfer Agent DMP-APTRZ

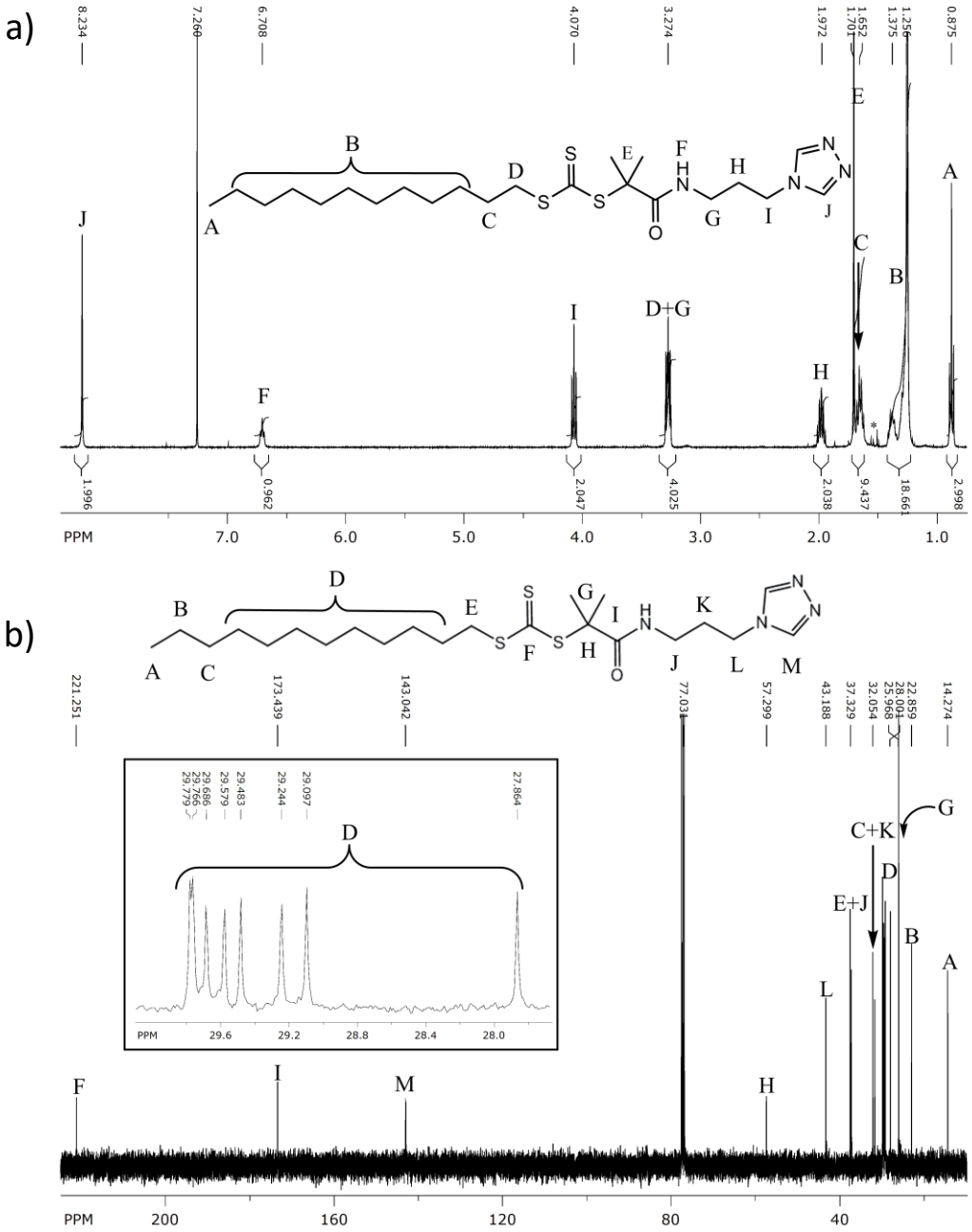

Figure S5: a) ^{1}H- (400 MHz) and b) ^{13}C-NMR (100 MHz) spectra of the triazole carrying chain transfer agent DMP-APTRZ, recorded in $CDCl_3$.

1.5.Triazole Monomer APTRZMAAm

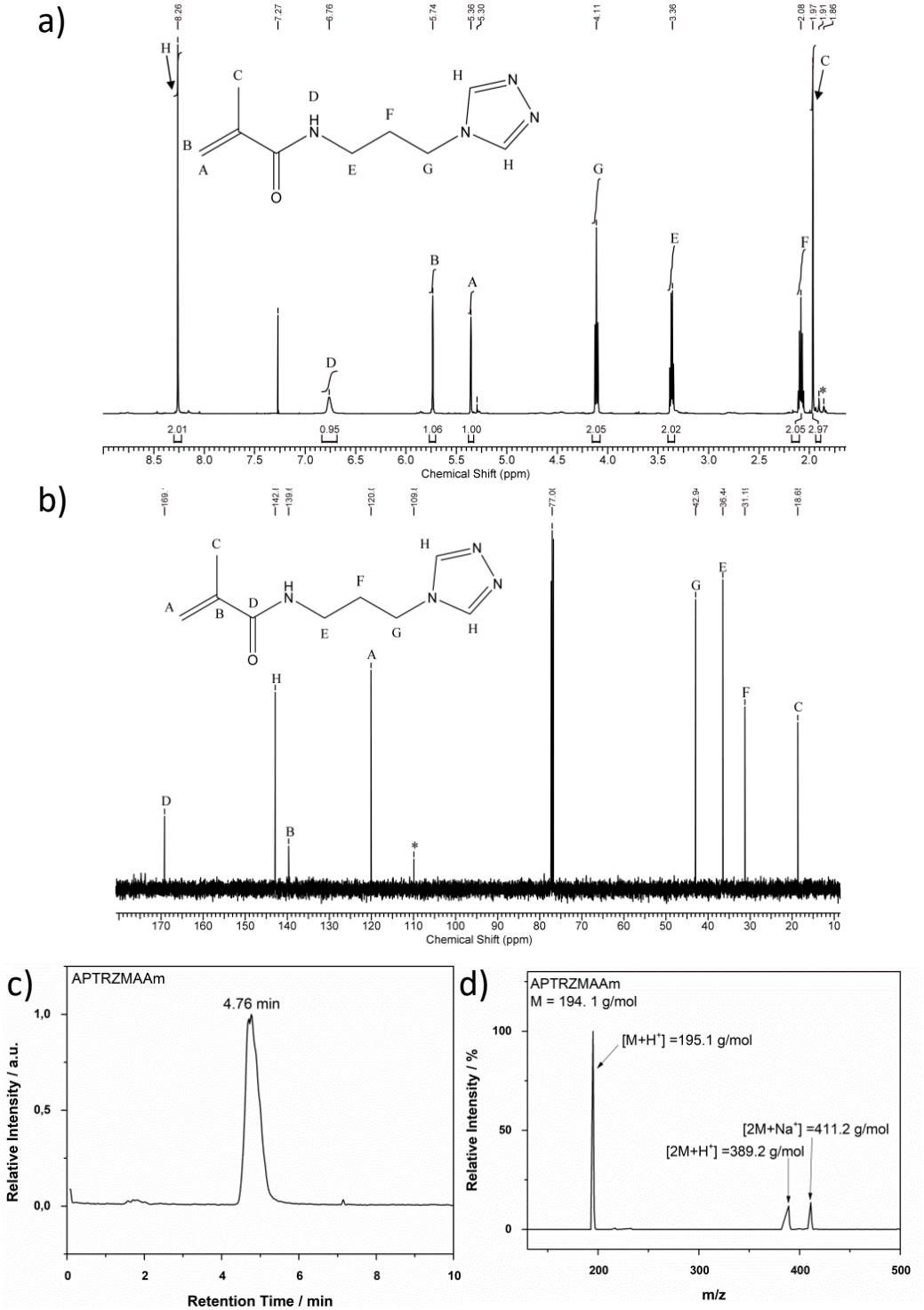

Figure S6: a) ^{1}H- (500 MHz) and b) ^{13}C-NMR (126 MHz) spectra of the triazole monomer APTRZMAAm, recorded in $CDCl_3$. Asterisks mark solvent residues. c) HPLC-MS chromatogram and d) mass spectrum of the corresponding product.

1.5.1. Failed Synthesis Route of APTRZAAm *via* Acryloyl Chloride

APTRZ (900 mg, 7.1 mmol) was dissolved in $CHCl_3$ (40 mL), containing K_2CO_3 (4.44 mg, 32.1 mmol). 2-Propenoyl chloride (1293 mg, 14.29 mmol) was dissolved in $CHCl_3$ (40 mL) and added dropwise to the cooled reaction mixture under vigorous stirring. The conversion was investigated by TLC (plate: Al_2O_3-N, eluent: CH_2Cl_2/ MeOH/ NH_3 (45:7:1), iodine indication, $R_{f,}$(APTRZAAm)=0.69). After 45 h the mixture concentrated *via* rotary evaporation and concentrated under vacuum. The remaining gel was diluted in DCM and filtered to remove the K_2CO_3 and concentrated to dryness. Afterwards the slight brownish oil was dissolved in water and freeze dried. The acrylic acid impurities were removed by column chromatography (cellulose MN 2100, Hexane) and the pure product was obtained by an eluent change (cellulose MN 2100, THF:EtCOOH = 28:1, iodine indicator, $R_{f,}$(APTRZAAm) = 0.81). The product phase was concentrated to dryness.

Yield: 486 mg (24%)

^{1}H-NMR (400 MHz, $CDCl_3$, shown in Figure S7A), δ ppm: 1.23 (t, 3H, R-COO-CH_2-C<u>H</u>$_3$), 2.25 (q, 2H, R-CONH-CH_2-C<u>H</u>$_2$-CH_2-R), 3.04 (t, 2H, R-CH_2-C<u>H</u>$_2$-COO-R), 3.35 (q, 2H, R-CONH-C<u>H</u>$_2$-CH_2-CH_2-R), 4.12 (q, 2H, R-COO-C<u>H</u>$_2$-CH_3), 4.59 (t, 2H, R-CONH-CH_2-CH_2-C<u>H</u>$_2$-TRZ), 4.73 (t, 2H, R-TRZ-C<u>H</u>$_2$-CH_2-R), 5.67 (dd, 1H, <u>H</u>CH=CH-CONH-R), 6.23 (dd, 1H, HC<u>H</u>=CH-CONH-R), 6.38 (dd, 1H, $_2$HC=C<u>H</u>-CONH-R), 8.62 (br. t, 1H, H_2C=CH-CON<u>H</u>-R), 9.24 (s, 1H, R-<u>TRZ</u>-R) and 10.43 (s, 1H, R-<u>TRZ</u>-R).

^{13}C NMR (101 MHz, $CDCl_3$, shown in Figure S7b): d ppm 14.0 (R-COO-CH_2-<u>C</u>H_3), 29.8 (R-TRZ-CH_2-<u>C</u>H_2-R), 32.4 (R-CONH-CH_2-<u>C</u>H_2-CH_2-R), 35.4 (R-CONH-<u>C</u>H_2-CH_2-CH_2-R), 46.3 (R-CONH-CH_2-CH_2-<u>C</u>H_2-TRZ), 48.1 (R-TRZ-<u>C</u>H_2-CH_2-R), 61.5 (R-COO-<u>C</u>H_2-CH_3), 126.2 ($_2$H<u>C</u>=CH-CONH-R), 131.0 ($_2$HC=<u>C</u>H-CONH-R), 143.9 (R-<u>TRZ</u>-R), 144.6 (R-<u>TRZ</u>-R), 166.9 ($_2$HC=CH-<u>C</u>ONH-R), 169.6 (R-CH_2-<u>C</u>OO-CH_2-CH_3).

The obtained product from this coupling reaction in chloroform (yield: 24–35 %) is shown below (Figure S7). It suggests a quarterisation of the targeted APTRZAAm-structure *via* aromatic nitrogen in the triazolyl group based on a Michael addition-like reaction, which results in an addition of a propionyl acetate rest to the five-membered triazole ring.

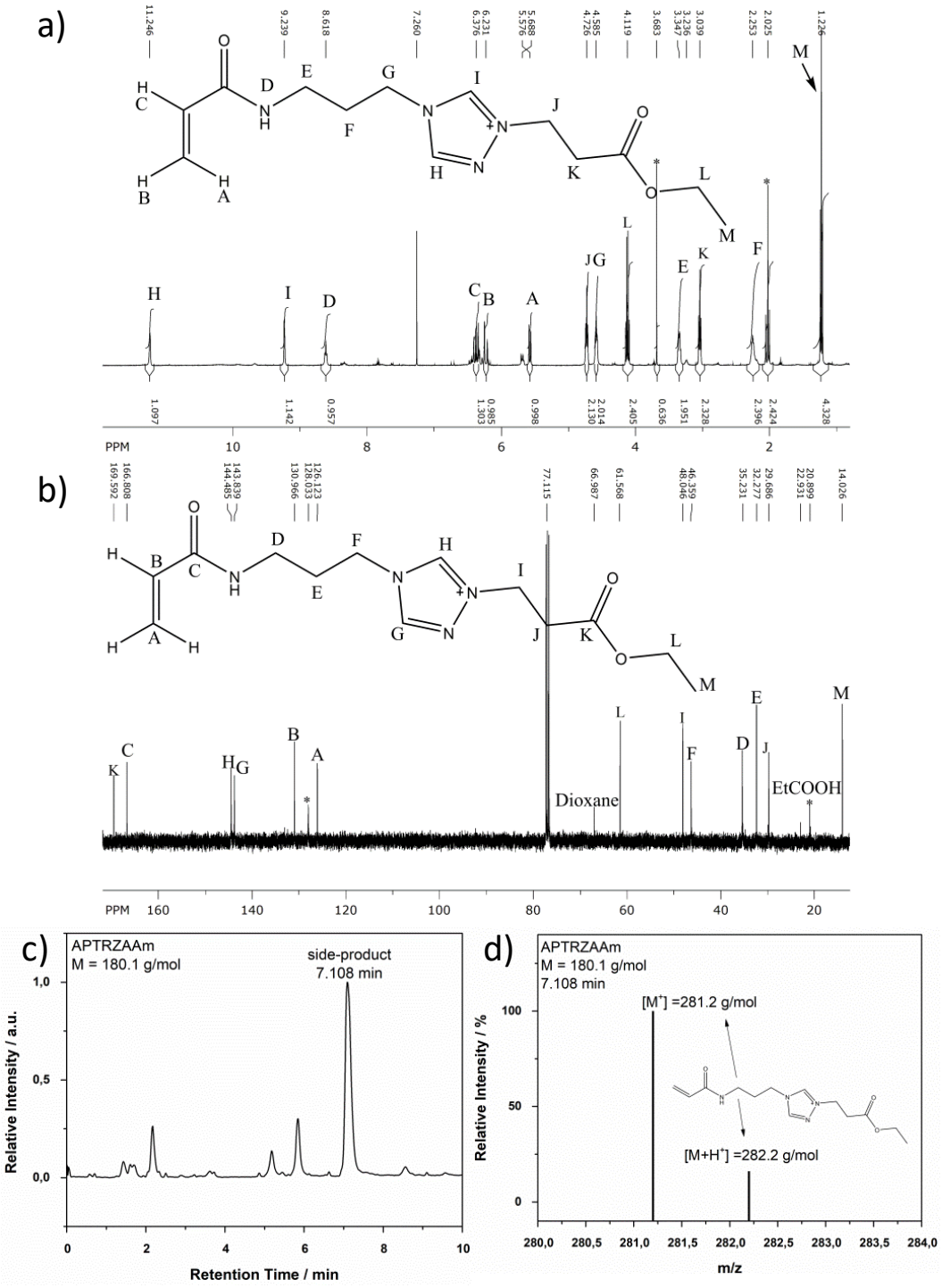

Figure S7: a) ^{1}H- (400 MHz) and b) ^{13}C- NMR (100 MHz) spectra of the Michael addition side product within the synthesis in chloroform of the monomer APTRZAAm, recorded in $CDCl_3$. Asterisks mark solvent residues (H_2O). c) HPLC-MS chromatogram and d) mass spectrum of the corresponding side product.

In dioxane, the coupling reaction led to the targeted product APTRZAAm, which underwent the Michael addition by forming a propionic acid rest at the triazole ring during the subsequent workup and column chromatography (Figure S8).

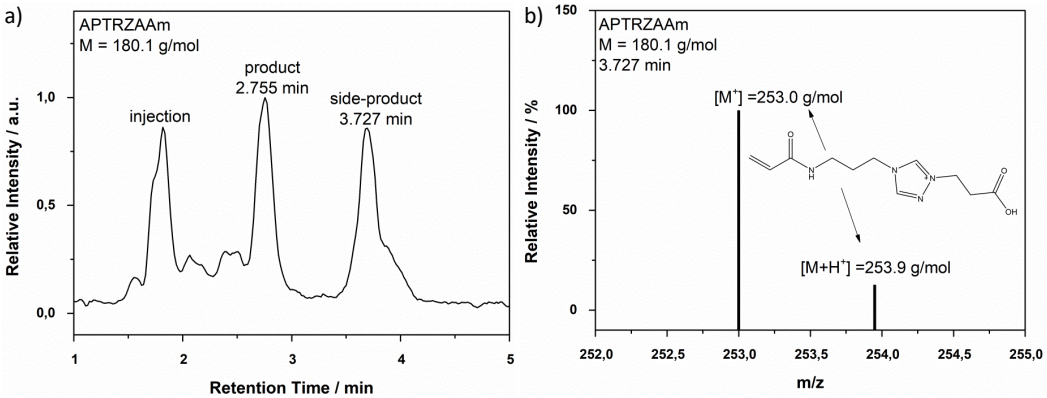

Figure S8: a) HPLC-MS chromatogram and b) mass spectrum of the Michael addition side product within the coupling reaction in dioxane of the target monomer APTRZAAm after short-column chromatography with acidic eluent.

Despite varied tested excesses of acryloyl chloride, a complete conversion could not be reached in respect of the educt APTRZ, so that the remaining APTRZ had to be subsequently separated. Extraction of the product (APTRZAAm) was not enabled due to the water-solubility of the educts K_2CO_3, AA, APTRZ and the product APTRZAAm. Also, column chromatography was not successful, independently of the choice of the stationary phase (Al_2O_3-N, cellulose Cell300, silica) and eluent mixture. The acidification of the eluent enabled the removal of APTRZ, but led to a formation of the Michael addition derivate from the addition of APTRZAAm and free acryloyl chloride. The assumption of an added propionyl acetate moiety was confirmed by TLC, HPLC-MS and NMR measurements (shown in Figure S7).
The added rest deviated in dependence of the chosen solvent. In chloroform, the pseudo Michael addition product was formed with a high conversion (visible in Figure S7 c/d). In acetonitrile, a reaction between the solvent and the educts seemed to take place. In freshly distilled dioxane, the product APTRZAAm is obtained in the coupling reaction (chemical equivalent trizaolyl protons were visible in ^{1}H NMR), but could not be purified (Figure S8a/b). During the separation of product and impurities *via* column chromatography (cellulose, eluent: EtOH/Hex/EtCOOH (200:100:1)) the pure product underwent the previous described side-reaction (visible in Figure S8a/b). The use of different bases (e.g. DMAP/TEA) complicated the purification dramatically.

1.5.2. Failed Synthesis Routes of APTRZAAm *via* EDC coupling and active Ester

EDC coupling: The APTRZ (100.0 mg, 1.03 mmol) was added to dichloromethane (100 mL) solution containing the excesses of 66 % EDC (296.5 mg, 1.55 mmol) and 10 % acrylic acid (74.3 mg, 1.03 mmol) under argon flux. 4-(Dimethylamino)-pyridine (125.8 mg, 1.03 mmol) was added to the above reaction mixture and stirred for one day at room temperature. The conversion was investigated by TLC (plate: Cell-300, eluent: EtOH/Hex/EtOOH (200:100:1), iodine and $FeBr_2$ indication). -Yield: 0 mg (0%)

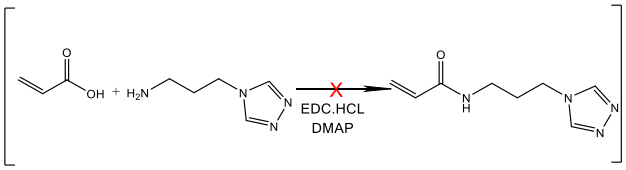

Scheme S1: Failed synthesis of APTRZAAm *via* EDC coupling.

Active ester: 2,5-Dioxopyrrolidin-1-yl acrylate (100 mg, 0.59 mmol) was dissolved in dry EtOAc (or $CHCl_3$) (12 mL). A solution of APTRZ (49.7 mg, 0.39 mmol) in $CHCl_3$ (10.5 mL) was added dropwise under vigorous stirring and formation of precipitation. The reaction mixture was diluted with dry EtOAc (10 mL) after 30 min reaction time. The conversion was investigated by TLC (plate: Al_2O_3-N, eluent: CH_2Cl_2/ MeOH/ NH_3 (45:7:1), iodine and $FeBr_2$ indication). After 45 h the mixture was concentrated *via* rotary evaporation and concentrated under vacuum. The remaining gel was diluted in DCM and filtered to remove the K_2CO_3 and concentrated to dryness. Afterwards the slight brownish oil was dissolved in water and freeze dried. -Yield: 0 mg (0%)

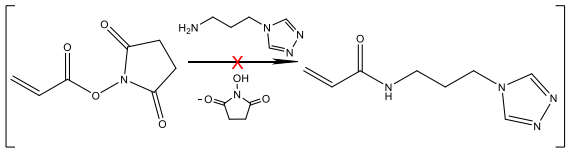

Scheme S2: Failed synthesis of APTRZAAm *via* active ester NAS.

The applied synthesis routes revealed the main difficulties of the synthesis of a triazole functionalized monomer based on APTRZ. The main educts and side products of the chosen routes are water-soluble, so that separation of the product was disabled. The incomplete conversion of the educt APTRZ to product APTRZAAm (similar solubilities) demanded a separation by column chromatography. A potential acidic eluent (protonation of the amine APTRZ) led to the Michael addition of the product.
The application of a methacrylic derivate avoided this addition. A coupling with DCC forms water-insoluble dicyclohexyl urea, which simplifies the work-up. Consequently, the route of APTRZMAAm *via* DCC coupling was preferred over the coupling trials above.

1.5.3. Failed Synthesis Routes of APTRZAAm *via* CDI coupling

The coupling was performed also with 3-amino-1,2,4-triazole (NH_2-TRZ), the purchasable analogue of APTRZ. The unsuccessful synthesis of APTRZAAm is explained in accordance to this exemplary reaction (scheme S3). The analogue side product was purified (shown in Figure S9). On the base of this analogue and its ^{1}H-NMR with impurities (not shown), the Michael addition side product of APTRZ (scheme 4) was anticipated.

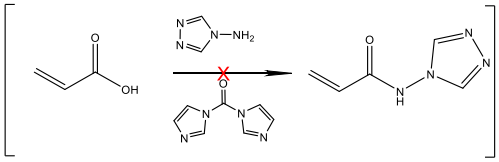

Scheme S3: Failed synthesis of NH_2-TRZAAm *via* CDI coupling.

CDI (925.6 mg, 5.70 mmol) was dissolved in distilled dioxane (20 mL) containing AA (342.8 mg, 4.78 mmol). TRZ-NH_2 (200.0 mg, 2.38 mmol) was added to the reaction mixture after 15 minutes under vigorous stirring. A whitish precipitate was obtained after short time. The solid was filtered and washed several times with distilled dioxane. The product was dissolved in little amount of distilled water and precipitated in EtOAc. The analyses revealed the formation of a side product. -Yield: 0 mg (0%)

The CDI forms an activated imidazolid species of AA as intermediate, which is supposed to react with amines under cleavage of an imidazole rest. The found product corresponds to the Michael addition-like product of this activated intermediate of this CDI coupling reaction (shown scheme S9). The side product precipitated once formed (whitish solid), which is insoluble in the most organic solvents. The obtained purified side product belongs to the suggested Michael addition product (Figure S9). On the base of this discussed analogue, the synthesis progress (and appearance) and its ^{1}H-NMR with impurities (not shown) the Michael addition side product of APTRZ (scheme 4) was anticipated.

CDI (308.6 mg, 1.90 mmol) was dissolved in distilled dioxane containing AA (114.3mg, 1.59 mmol). After 15 minutes APTRZ (100 mg, 0.79 mmol) was dissolved in distilled dioxane (1 mL) and added to the previous mixture. A whitish precipitate was obtained after short time. The solid was filtered and washed several times with distilled dioxane. The product was dissolved in little amount of distilled water and precipitated in EtOAc. The analyses revealed the formation of a side product. -Yield: 0 mg (0%)

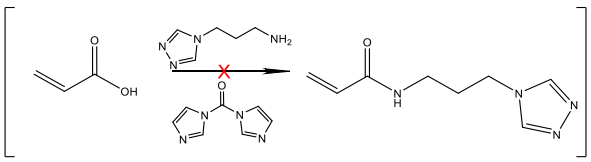

Scheme S4: Failed synthesis of APTRZAAm *via* CDI coupling.

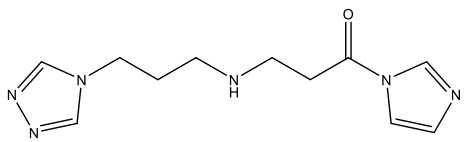

Scheme S5: Anticipated side product of the failed synthesis of APTRZAAm *via* CDI coupling in accordance to its ^{1}H-NMR with impurities (not shown) and the shown purified analogue *via* NH_2-TRZ coupling.

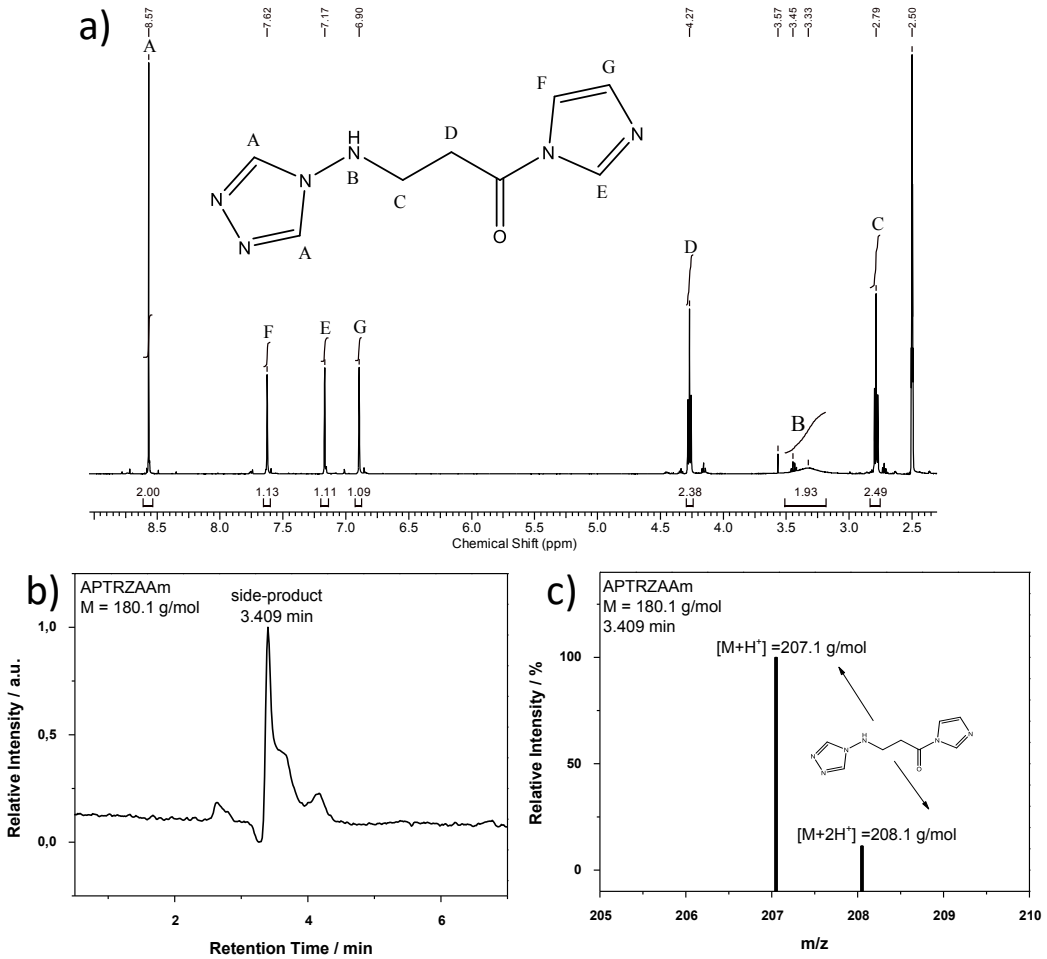

Figure S9: a) ^{1}H- NMR (400 MHz) spectrum of the Michael addition product within the synthesis of the comparable monomer NH_2-TRZAAm with NH_2-TRZ as coordinating functionality, recorded in DMSO-d_6. b) HPLC-MS chromatogram and c) mass spectrum of the corresponding side product.

1.6. Hemi-Telechelic and Multidentate Macromolecular Coordination Ligands

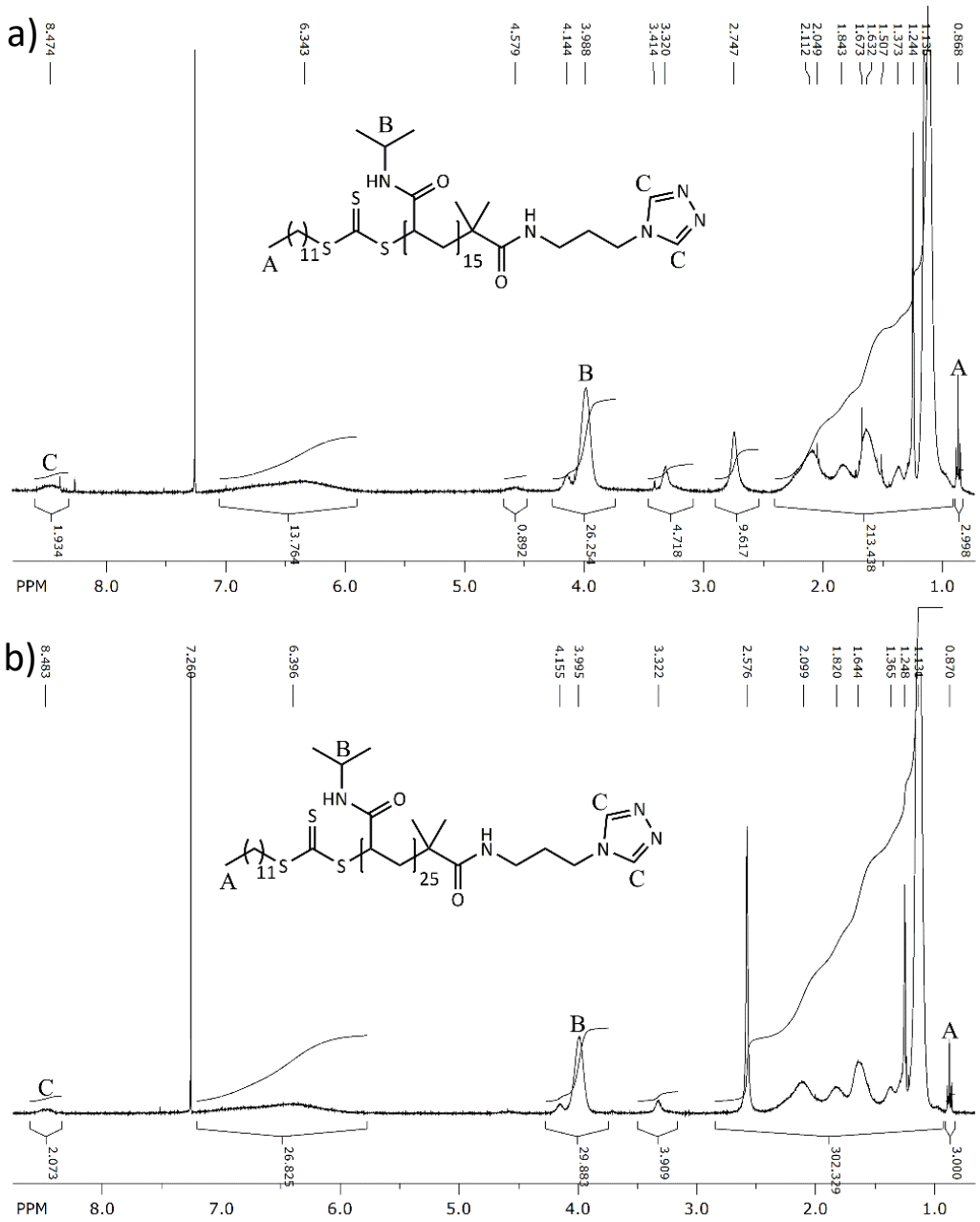

Figure S10*:* Exemplary ^{1}H-NMR (400 MHz) spectra of the hemi-telechelic MCLs **P3k** (a) and **P4k** (b), recorded in $CHCl_3$.

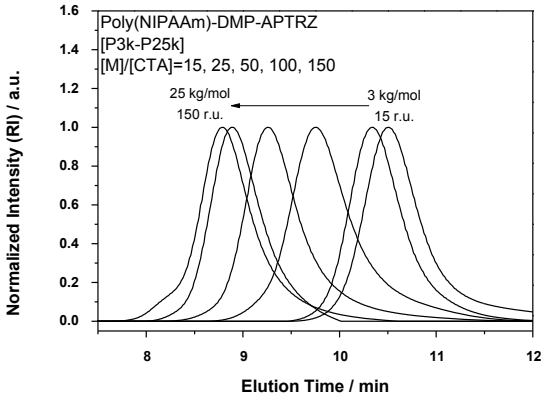

Figure S11: Exemplary GPC elugrams of the hemi-telechelic MCLs **P3k** – **P23k**.

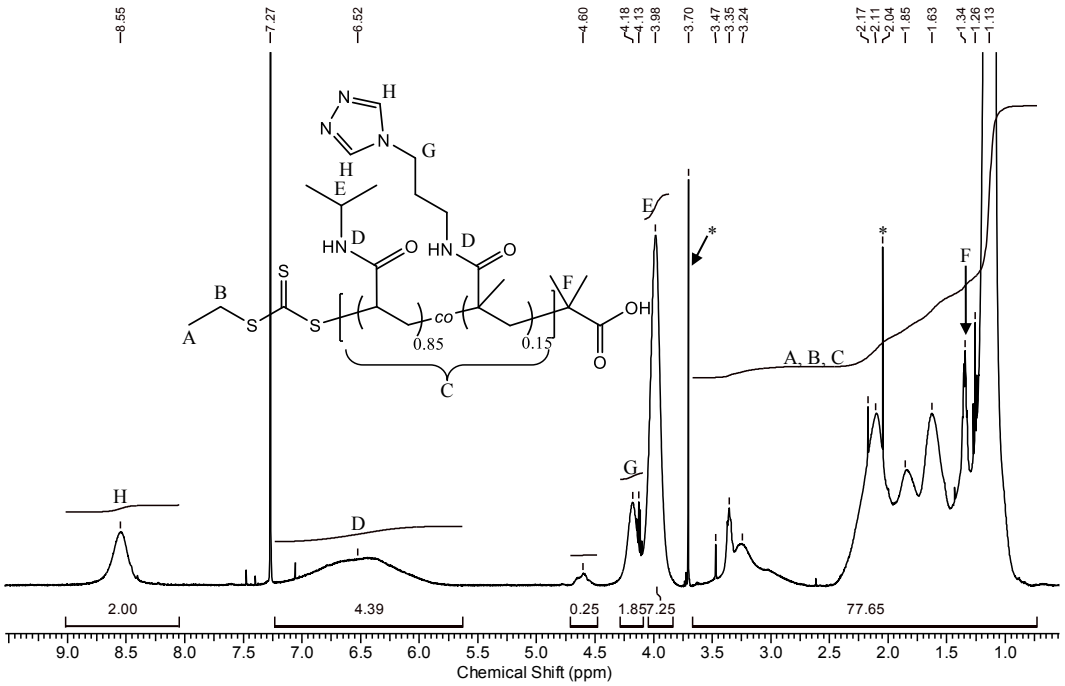

Figure S12: Exemplary ^{1}H-NMR (400 MHz) spectrum of the multidentate MCLs **C4.6k15%**, recorded in $CHCl_3$. Asterisk mark solvent residues.

2. Aggregation Studies

2.1. Turbidity Measurement of Hemi-Telechelic Macromolecular Coordination Ligands

Table S1: Cloud point temperatures (T_c) and apparent hydrodynamic diameters (D_h) of the MCLs as determined by DLS in dependence of molar mass ($\bar{M}_n$) at 22 and 35 °C in water and Fe^{2+} solution.

sample code	$\bar{M}_n$ /kg·mol^{-1}	H_2O			Fe^{2+}_{aq}		
		T_c[c] / °C	$D_{h,22C°}$ / nm	$D_{h,35°C}$ / nm	T_c[c] / °C	$D_{h,22C°}$ / nm	$D_{h,35C°}$ / nm
P3k[a]	3.1	34.7	md.[b]	652	30.2	md.[b]	1855
P4k[a]	3.9	33.4	md.[b]	316	32.2	15, 1107	1375
P7k	6.9	32.9	18, 108	186	31.5	20, 126	2335
P12k	12.3	34.1	20	150	33.2	20	1951
P23k	23.3	34.8	21	117	33.4	21	1990

[a] The polymers precipitates as consequence of the addition of iron.
[b] Multiple aggregation size distributions were observed.
[c] The values were extracted from the heating cycle.

2.2. DLS of Hemi-Telechelic Macromolecular Coordination Ligands

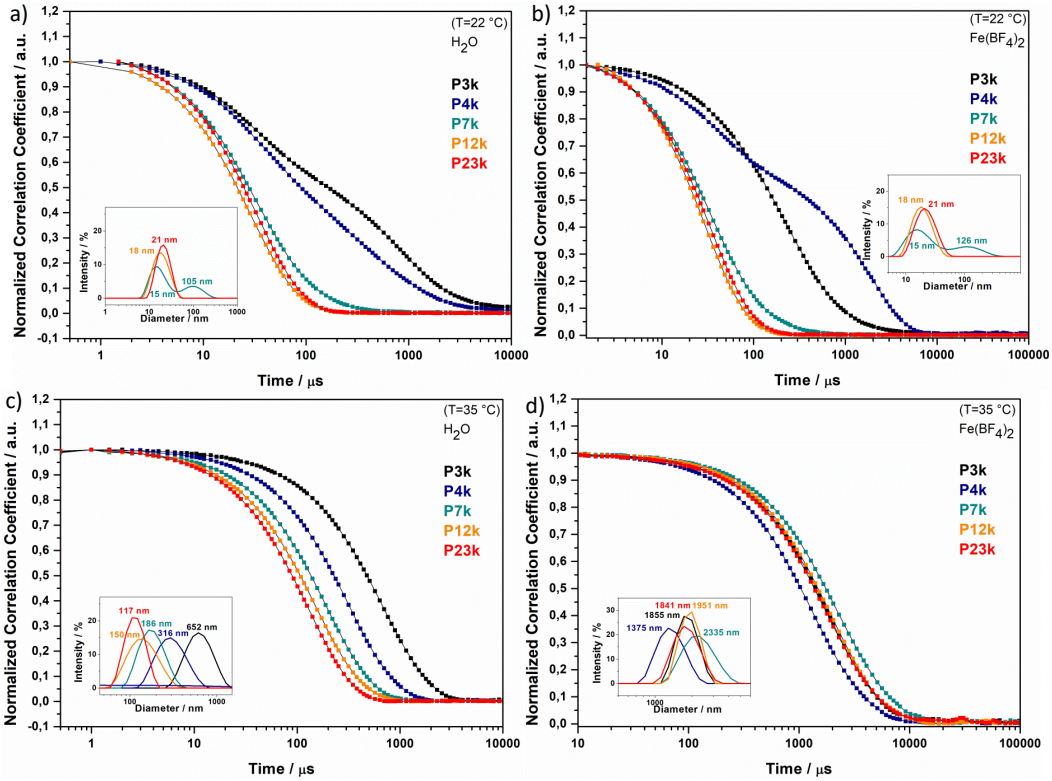

Figure S13: DLS measurement of a 0.1 wt% polymer solution for the determination of the iron-ion-sensitive aggregation behaviour of the hemi-telechelic MCLs **P3k** - **P23k** in dependence of their molar mass with the (apparent) hydrodynamic diameter in aqueous medium (a, c) and with tenfold Fe^{2+} excess (b, d), below (a-b) and above (c-d) the T_c.

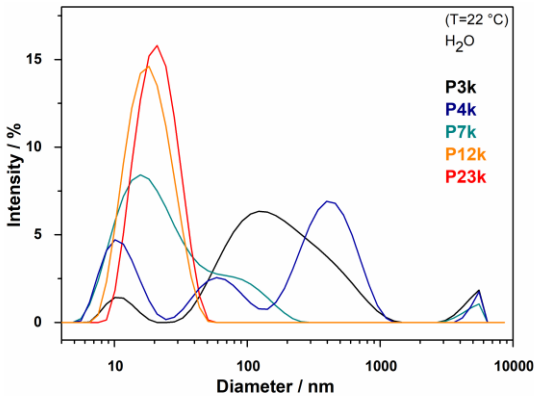

Figure S14: The chain length dependence of the aggregation size of the hemi-telechelic MCLs **P3k** - **P23k** in pure aqueous solution with a 0.1 wt% polymer solution below (22 °C) the T_c.

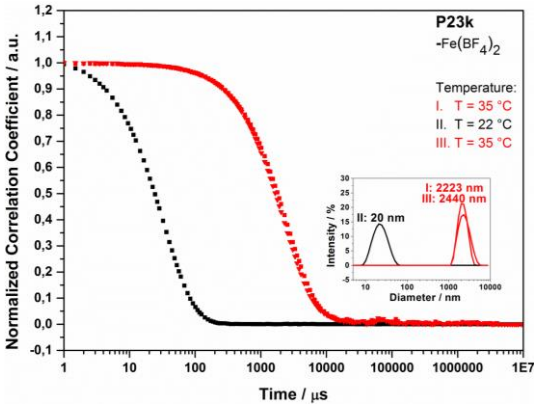

Figure S15: DLS measurement below (22 °C) and above (35 °C) the T_c to demonstrate the reversibility of the temperature-controlled aggregation behaviour of the MCL **P23k** (0.1 wt% polymer solution) with tenfold excess of Fe^{2+} ions.

2.3. TEM Imaging of Hemi-Telechelic Macromolecular Coordination Ligand P23k

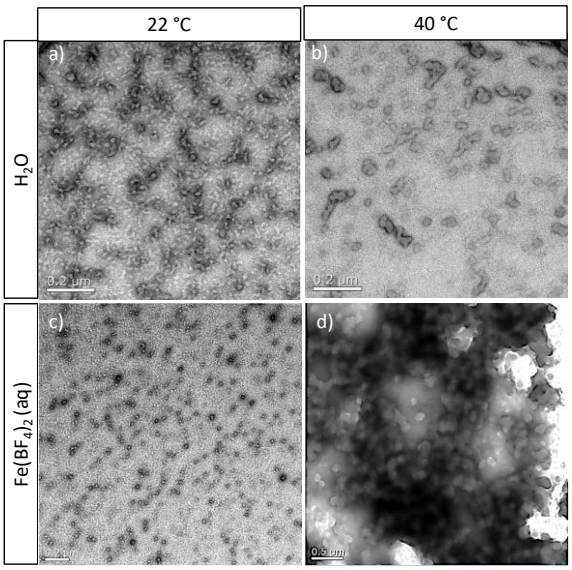

Figure S16: Exemplary TEM images of the long hemi-telechelic MCL **P23k** in threalose matrix prepared from a 0.1 wt% aqueous solution under varying conditions.

In pure water below the critical solution temperature (T=22 °C) **P23k** forms truncated wormlike aggregates of 10 nm diameter and length of up to 50 nm (similar range to DLS data, Figure 2), with very broad length distribution and irregular shape (Figure S16a). Above the cloud point (T=40 °C), globular aggregates with increased dimensions (average around 100 nm, broad distribution, matching DLS data, Figure 2) and irregular shape are formed, which tend to cluster (Figure S16). An increased hydrophobicity of and stronger affinity between the polymer chains above T_c would explain this behaviour. In solution with iron ions (T=22 °C) below the T_c, the long polymer **P23k** forms highly spherical aggregates with highly spherical geometry and diameters of about 10 nm (Figure S16c, congruent with DLS data, Figure 2). Probably, Fe^{2+} addition leads to a slight compaction of the aggregates from pure water, but probably due to the large polymer chain, extended 1D complexes cannot form under these conditions. Above T_c (at T=37 °C) in presence of iron ions, **P23k** forms larger, slightly elongated aggregates with globular shape of 100-600 nm diameter and strong tendency to cluster (Figure S16d, note the larger scale bar of 0.5 µm), explaining also the large increase in correlation time in DLS (Figure 2). Here, the collapsed polymer chains have less space requirement and may facilitate Fe^{2+} coordination to larger structures.

2.4. DLS of Multidentate Macromolecular Coordination Ligands

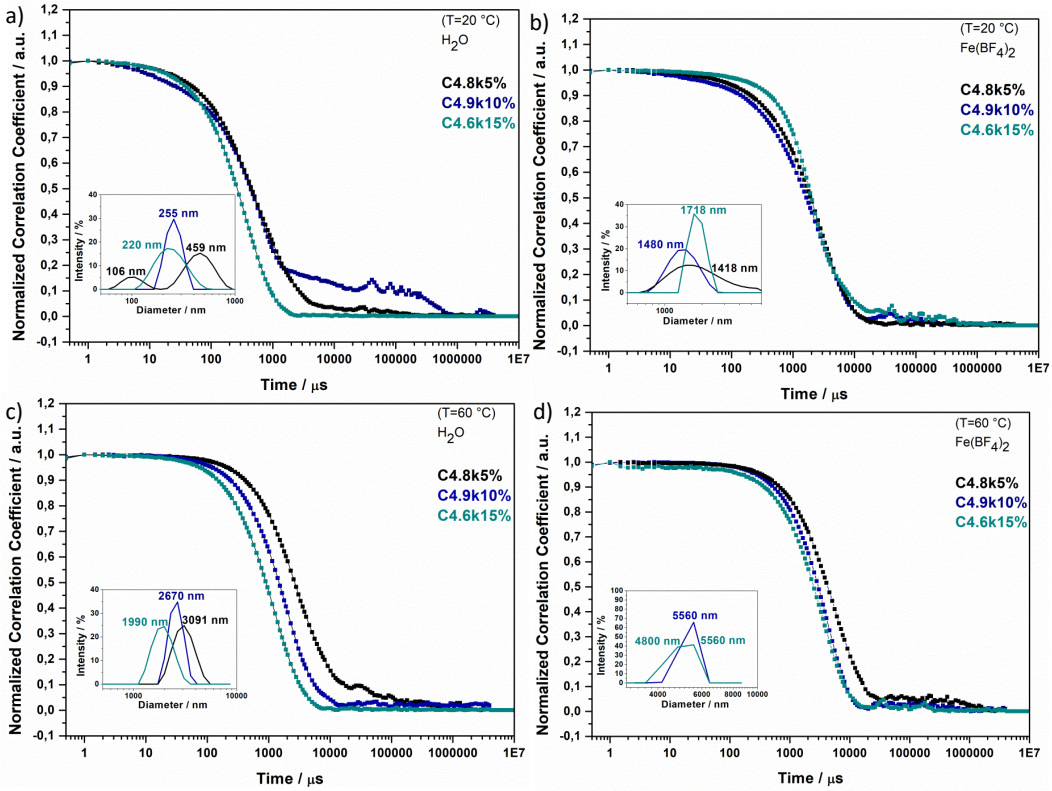

Figure S17: DLS measurement for the determination of the iron-ion-sensitive aggregation behaviour of the multidentate MCLs **C4.8k5%**, **C4.9k10%** and **C4.6k15%** in dependence of their APTRZMAAm content within the copolymer with their (apparent) hydrodynamic diameter in aqueous solution without (a, c) and with Fe^{2+} (b, d) solution with a tenfold excess, below (a-b) and above (c-d) the T_c of an 1 wt% polymer solution.

3. Overview Scheme

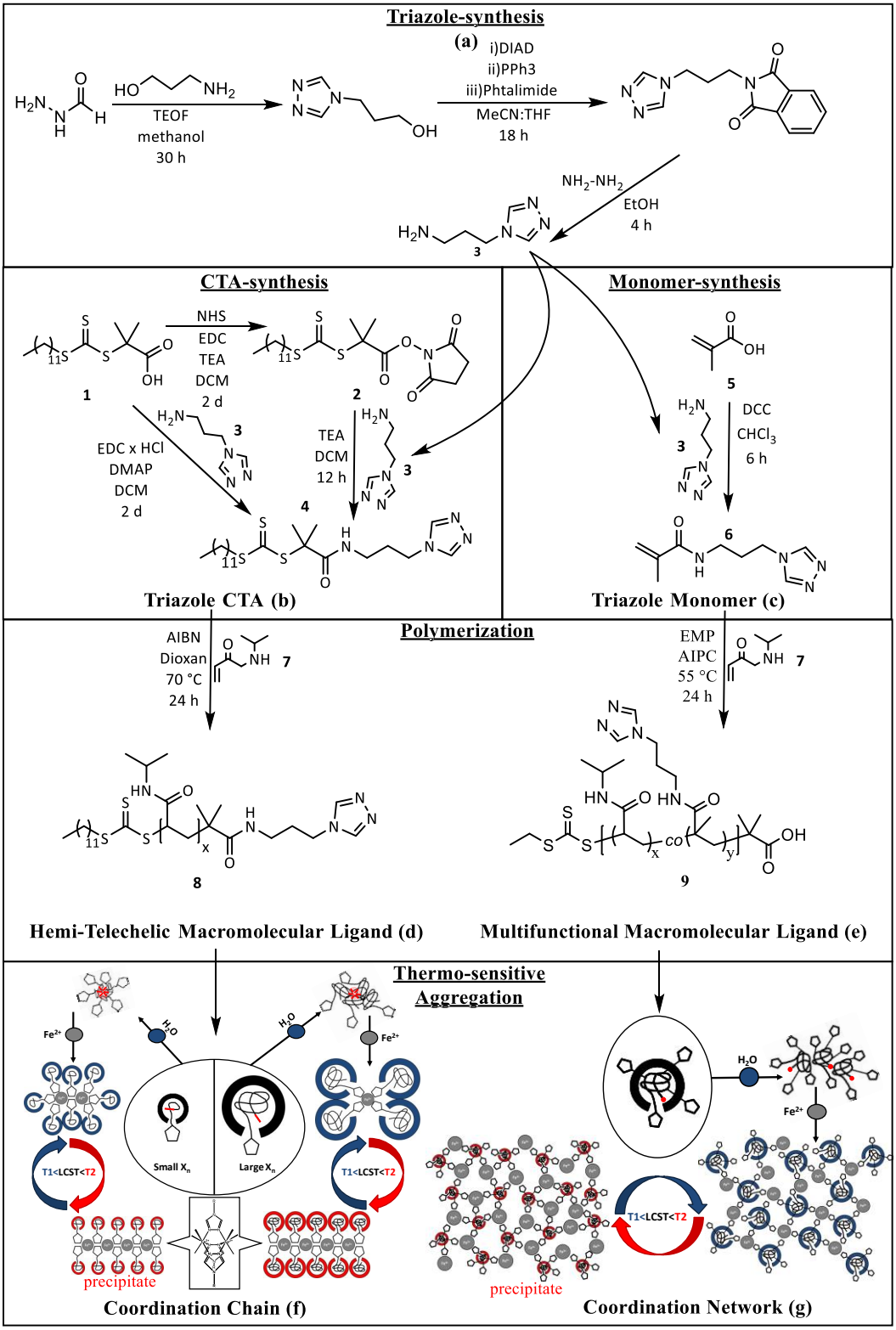

Figure S18: Flow diagram of the syntheses and the corresponding aggregation studies in dependence of the two ligand architectures for (d) hemi-telechelic and (g) multidentate macromolecular coordination ligands.